# 3

# Mitigation of Destabilizing Effects of CPL in a Buck Converter Feeding a Mixed Load

The Chapter 2, addressed mitigation of the destabilizing effects of CPLs in dc/dc boost converter based equivalent dc distribution system using SMC approach. This chapter deals with mitigation of the CPL induced negative impedance instabilities in a dc/dc buck converter. A buck converter is usually used in a dc distribution system to step-down the dc voltage, either to extend the primary distribution for low voltage applications or to meet a specific low voltage requirement of a load. The system considered in this chapter consists of a dc/dc buck converter feeding a realistic load profile consisting of resistive and CPL components, representing a buck converter based equivalent dc distribution system with tightly-regulated POLC. Nonlinear switching function based discontinuous and PWM based sliding mode controllers are proposed to mitigate CPL induced instabilities (e.g. limit cycle oscillations and voltage collapse) and to ensure output voltage regulation. The existence of the sliding mode and stability of the switching surface have been proved analytically. The effectiveness of the controllers has been validated using simulation studies and experimental results.

## 3.1 MATHEMATICAL MODELING OF BUCK CONVERTER WITH MIXED LOAD

The circuit diagram of a non-isolated dc/dc buck converter feeding a mixed load (CPL and CVL) is shown in Figure 3.1. The converter is assumed to operate in CCM. Now considering the circuit diagram of Figure 3.1, the total instantaneous current drawn from the load bus is given by

$$i_{bus}(t) = \frac{v_{bus}(t)}{R_L} + \frac{P}{v_{bus}(t)}; \quad \forall \;\; v_{bus}(t) > \varepsilon \tag{3.1}$$

that is,

$$i_{bus}(t) = i_{Load}(t) = i_{CPL} + i_{CVL} \tag{3.2}$$

where $P$ is the rated power of the CPL, $R_L$ is the resistance of the CVL, $i_{CPL}$ is the current drawn by the CPL, $i_{CVL}$ is the current drawn by the CVL, $v_{bus}$ is the voltage at the load bus ($v_C$=$v_0$=$v_{bus}$) i.e., output voltage $v_0$ of the buck converter and $\varepsilon$ is a small positive value.

The state-space averaged model of the system shown in Figure 3.1 is given by

$$\frac{dx_1}{dt} = \frac{E}{L}u - \frac{1}{L}x_2 \tag{3.3a}$$

$$\frac{dx_2}{dt} = \frac{1}{C}x_1 - \frac{1}{C}i_{Load} \tag{3.3b}$$

$$v_0 = x_2 \tag{3.3c}$$

where $x_1$ and $x_2$ are the moving averages of inductor current $i_L$, and capacitor voltage $v_C$ respectively. $E$ is the input voltage of the converter. $L$ and $C$, are converter's inductance and capacitance parameters respectively. $u \in \{0,\ 1\}$, is the control input. Furthermore, $x_1$, $x_2 \in \Omega$, where set $\Omega$ is a subset of $\mathbb{R}^2$ i.e.

$$x_1, x_2 \in \Omega \subseteq \ \mathbb{R}^2_+ \setminus \{0\} \ \textit{and} \ x_1 > 0,\ x_2 > 0 \tag{3.4}$$

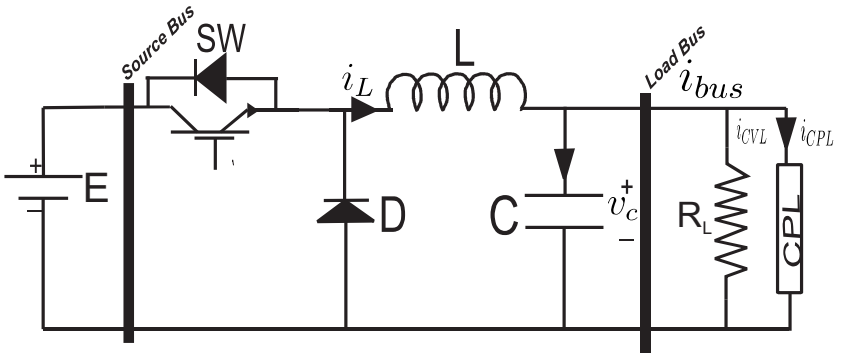


**Figure 3.1 :** Circuit diagram of a DC/DC converter feeding a combination of CPL and CVL

The parasitic components, inductor's series resistance and capacitor's Equivalent Series Resistance (ESR) etc., increase the effective damping of the system, and can provide damping to oscillations induced due to negative impedance instabilities [Huddy and Skufca, 2013]. Therefore, to consider a worst case scenario, from the stability point-of-view, an ideal model of the converter is considered. Therefore, with these assumptions the designed controller would be subjected to the most severe situation of negative impedance instabilities in the system.

## 3.2 SLIDING MODE CONTROL DESIGN

In this section, a discontinuous (variable switching frequency) and PWM based SMCs are proposed for the dynamic model defined in (3.3). Limit on total power to ensure stability is also computed.

### 3.2.1 Discontinuous SMC

In this subsection, the modified nonlinear switching function to design a discontinuous SMC is introduced, followed by definition of a control law, which brings sliding mode in finite time. The discontinuous SMC has variable switching frequency, which may reach a very high value to maintain sliding mode. However, discontinuous SMC ensures high degree of robustness as sliding mode $s = 0$ is maintained.

#### *(a) Nonlinear switching function*

The first step in the design of a sliding-mode controller for a given system is to design a stable switching function. The following nonlinear switching function proposed in Chapter 2, is used to design discontinuous SMC for the buck converter system of Figure 3.1

$$s := x_1 x_2 - x_{1ref} x_{2ref} + \mu(x_2 - x_{2ref}) \tag{3.5}$$

where $x_{1ref}$ and $x_{2ref}$ are the reference values of state variables $x_1$ and $x_2$ respectively. And $\mu > 0$ is the parameter of the switching function to control the convergence speed. The switching function is chosen to satisfy the objectives of constant power supply to the CPL and the output voltage regulation. It will be proved in subsequent sections that, when sliding mode is established ($s = 0$), the controller would ensure supply of constant power to the CPL and regulation of the dc bus voltage to a desired value.

In the second step, a control law is designed which forces the system trajectory on to the switching surface $s = 0$ and constrains it to the switching surface then on. The discontinuous control law is defined by

$$u := \frac{1}{2}(1 - sgn(s)) = \begin{cases} 0 & \text{if } s > 0 \\ 1 & \text{if } s < 0 \end{cases} \tag{3.6}$$

However, direct use of the above control law causes the converter to undergo switching at very high frequencies, which may not be desirable in practical situations. For the practical implementation purpose, the above control law can be modified to limit the highest switching frequency of the converter. In what follows next, proof of the existence of sliding mode is presented.

***(b) Existence of sliding mode***

It is essential that trajectory starting from an arbitrary initial condition reaches switching surface ($s=0$) in finite time, and is constrained to the surface then on. The designed control law must ensure reachability condition. The reachability condition is proved in the following theorem.

**Theorem** 3.1. The control law

$$u := \frac{1}{2}(1 - sgn(s)) \tag{3.7}$$

with the switching function $s := x_1x_2 - x_{1ref}x_{2ref} + \mu(x_2 - x_{2ref})$ ensures that reachability condition

$$s^T\dot{s} < -\eta\ |s| \tag{3.8}$$

for some $\eta > 0$, is satisfied when total load power $P_T$ satisfies

$$P_T < x_1x_2 + \frac{x_2^2C}{(x_1+\mu)L}(E - x_2) \tag{3.9}$$

where total load power $P_T$ is given by $P_T = P + \frac{x_{2ref}^2}{R_L}$.

**Proof:** To prove the theorem, two distinct cases are considered; Case I, when $s<0$, and Case II, when $s>0$. From the reachability condition, when $s<0$, it is to be ensured that $\dot{s}>0$ and vice versa.

**Case I:** $s<0$

$s<0$ implies $s := x_1x_2 - x_{1ref}x_{2ref} + \mu(x_2 - x_{2ref}) < 0$, and the control law (3.6) becomes 1. It is to be ensured that $\dot{s}>0$ with the control law (3.6) and model given in (3.3). That is

$$x_1\dot{x_2} + x_2\dot{x_1} + \mu\dot{x_2} > 0 \tag{3.10}$$

Substitution of $\dot{x_1}$ and $\dot{x_2}$ from (3.3) and subsequent algebraic manipulation gives

$$x_1(\frac{x_1}{C} - \frac{x_2}{CR_L} - \frac{P}{Cx_2}) + x_2(\frac{E}{L} - \frac{x_2}{L}) + \mu(\frac{x_1}{C} - \frac{x_2}{CR_L} - \frac{P}{Cx_2}) > 0 \tag{3.11}$$

Which leads to

$$(x_1+\mu)(\frac{x_1}{C} - \frac{x_2}{CR_L} - \frac{P}{Cx_2}) + \frac{x_2E}{L} - \frac{x_2^2}{L} > 0 \tag{3.12}$$

It implies

$$P_T < x_1x_2 + \frac{x_2^2C}{(x_1+\mu)L}(E - x_2) \tag{3.13}$$

**Case II:** $s>0$

$s>0$ implies $x_1x_2 - x_{1ref}x_{2ref} + \mu(x_2 - x_{2ref}) > 0$, and the control law (3.6) becomes 0. It is to be ensured that $\dot{s}<0$ with the control law (3.6) and model given in (3.3). That is

$$x_1\dot{x_2} + x_2\dot{x_1} + \mu\dot{x_2} < 0 \tag{3.14}$$

Substitution of $\dot{x_1}$ and $\dot{x_2}$ in the above equation and subsequent algebraic manipulation gives

$$x_1(\frac{x_1}{C}-\frac{x_2}{CR_L}-\frac{P}{Cx_2})+x_2(-\frac{x_2}{L})+\mu(\frac{x_1}{C}-\frac{x_2}{CR_L}-\frac{P}{Cx_2})<0 \tag{3.15}$$

Which leads to

$$(x_1+\mu)(\frac{x_1}{C}-\frac{x_2}{CR_L}-\frac{P}{Cx_2})-\frac{x_2^2}{L}<0 \tag{3.16}$$

Therefore, to ensure $\dot{s}<0$ the following condition should be satisfied.

$$P_T > x_1x_2-\frac{x_2^3C}{(x_1+\mu)L} \tag{3.17}$$

For the high voltage dc/dc converters upto few kilowatt rating $x_2>>x_1$. Furthermore, the right hand side of (3.17) is a small positive or negative number. Therefore, it is straight forward to satisfy (3.17). It is intuitive that the right hand side of (3.17) would be negative when $\mu=x_2$ and becomes more negative for decreasing values of $\mu<x_2$ and moves towards zero for increasing value of $\mu>x_2$. It implies that the equation (3.17) will always be satisfied by appropriate selection of $\mu$. The region of existence of the sliding mode is constituted from the locus points in the state-space which satisfy (3.13) and (3.17). The region of existence of sliding mode for a particular simulated case is shown in Figure 3.4, in the section on simulation studies. This completes the proof.

### *(c) Stability during sliding mode*

In this section, it is proved that $x_1$ converges to $x_{1ref}$ and $x_2$ converges to $x_{2ref}$, when $s=0$ is ensured. The stability of the system at switching surface $s=0$ is proved by the following theorem, using Lyapunov approach.

**Theorem** 3.2. During sliding mode $s=0$, the system dynamics is asymptotically stable i.e. $x_1$ approaches to $x_{1ref}$ and $x_2$ approaches to $x_{2ref}$.

**Proof:** Let the following be defined as,

$$e_1 := (x_1-x_{1ref}) \tag{3.18a}$$

$$e_2 := (x_2-x_{2ref}) \tag{3.18b}$$

$$e_p := x_1x_2-x_{1ref}x_{2ref} \tag{3.18c}$$

It is easy to verify that $\dot{e_1}=\dot{x_1}$ and $\dot{e_2}=\dot{x_2}$. $e_1$, $e_2$ and $e_p$ represent the error in the inductor current, error in the output voltage and error in the power.
Using (3.3b), (3.5), and (3.18)

$$\dot{e_2}=\frac{x_{1ref}x_{2ref}+e_p}{C(e_2+x_{2ref})}-\frac{(e_2+x_{2ref})}{CR_L}-\frac{P}{C(e_2+x_{2ref})} \tag{3.19}$$

$$s=e_p+\mu e_2 \tag{3.20}$$

Sliding mode s=0, implies

$$e_p=-\mu e_2 \tag{3.21}$$

Thus, when $e_2\to 0$ as $t\to\infty$, it ensures $e_p\to 0$ as $t\to\infty$, and both these together imply that $e_1\to 0$ as $t\to\infty$
Using (3.19) and (3.21)

$$\dot{e_2}=\frac{(x_{1ref}x_{2ref}-P-\frac{x_{2ref}^2}{R_L})}{C(e_2+x_{2ref})}-\frac{(\mu R_Le_2+e_2^2+2x_{2ref}e_2)}{CR_L(e_2+x_{2ref})} \tag{3.22}$$

however, $x_{1ref}x_{2ref} = P_T$, which implies $(x_{1ref}x_{2ref} - P - \frac{x_{2ref}^2}{R_L}) = 0$. With this (3.22) reduces to,

$$\dot{e_2} = -e_2 \frac{(\mu R_L + e_2 + 2x_{2ref})}{CR_L(e_2 + x_{2ref})} \tag{3.23}$$

Equations (3.18b) and (3.21) imply that the stability of $e_2$ dynamics ensures stability of $e_p$ and $e_1$. Therefore, it is to be proved that dynamics of $e_2$ is stable. To prove stability of $e_2$, the following Lyapunov function is defined

$$V(e_2) = \frac{1}{2}e_2^2 \tag{3.24}$$

The derivative of (3.24) is given by

$$\dot{V}(e_2) = e_2\dot{e_2} \tag{3.25}$$

Using (3.23), (3.25) implies

$$\dot{V}(e_2) = -e_2^2(\frac{\mu R_L + e_2 + 2x_{2ref}}{CR_L(e_2 + x_{2ref})}) \tag{3.26}$$

Using (3.18b),

$$\frac{\mu R_L + e_2 + 2x_{2ref}}{CR_L(e_2 + x_{2ref})} = \frac{\mu R_L + x_2 + x_{2ref}}{CR_L x_2} > 0 \tag{3.27}$$

where $\mu$, $x_2$, $x_{2ref}$, $R_L \in R_+ \setminus \{0\}$. Therefore, using (3.27), the right hand side of (3.26) becomes

$$\implies -e_2^2 \frac{\mu R_L + e_2 + 2x_{2ref}}{CR_L(e_2 + x_{2ref})} < 0 \tag{3.28}$$

It implies

$$\dot{V}(e_2) < 0 \tag{3.29}$$

Therefore, the system dynamics at switching function $s = 0$ is stable as $\dot{V}(e_2) < 0$, i.e. $x_1$ approaches to $x_{1ref}$ and $x_2$ approaches to $x_{2ref}$. This completes the proof.

The implementation scheme of the proposed discontinuous SMC for dc/dc buck converter system is shown in Figure 3.2.

### 3.2.2 PWM Based SMC

In case of discontinuous SMC, the switching frequency is variable and may become very high causing excessive losses. Moreover, in practical situations power converters can operate only at a finite switching frequency. Particularly, controllers designed through conventional SMC may not be suitable where a constant switching frequency is required. Furthermore, with variable switching frequency the design of circuit and filter components of the converter becomes problematic. One of the frequently used techniques in SMC to ensure fixed frequency operation is to use equivalent control approach. Details of the other methods used for chattering and frequency reduction can be found in [Cardoso et al., 1992; Tseng and Chen, 2010; Lee and Utkin, 2007], and the references therein.

In this section, a PWM based sliding mode controller, designed through reaching dynamics approach, is proposed for the buck converter system of (3.1). The following reaching dynamics is chosen to derive the instantaneous duty cycle $u(t)$ of the buck converter

$$\dot{s} = -\lambda\ s - Qsgn(s) \tag{3.30}$$

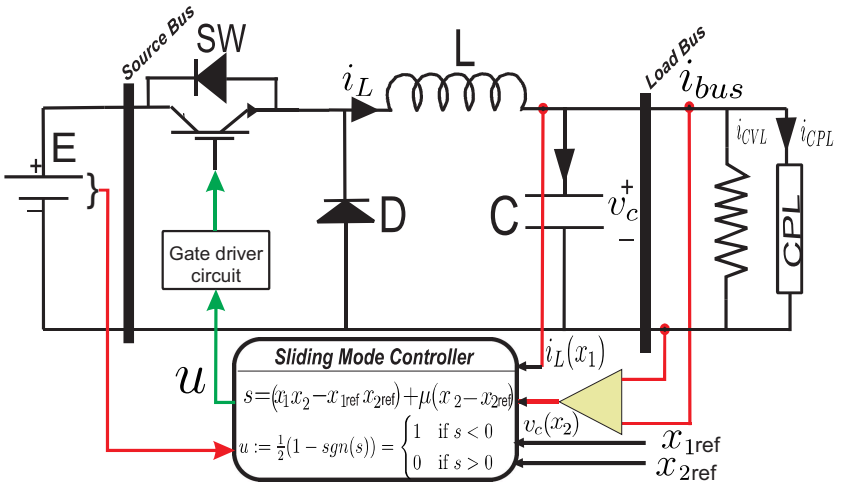


**Figure 3.2 :** Implementation scheme of the proposed discontinuous SMC for buck converter feeding a mixed load

where $\lambda$, $Q > 0$ are the parameters of the reaching dynamics to control the convergence speed of the switching function. Using (3.3), (3.5) and (3.30) and solving for $u(t)$ gives the following instantaneous duty cycle expression

$$u(t) = \frac{x_2}{E} - \frac{(x_1+\mu)L}{CEx_2}(x_1 - i_{Load}) - \frac{\lambda\ L\ s}{x_2 E} - \frac{QLsgn(s)}{x_2 E} \tag{3.31}$$

In the above equation, the last term represents discontinuous control designated as $u_N$. The first three terms combined together represent equivalent control $u_{eq}$. It decomposes the control law (3.31) as,

$$u(t) = u_{eq} + u_N \tag{3.32}$$

where $u_{eq}$ is the equivalent control law and represents a continuous approximation of the switching control law of discontinuous SMC at $s = 0$, and $u_N$ is the discontinuous part which ensures robustness to the parameter uncertainties and external disturbances in reaching phase. The value of constant $Q$ in (3.31) should be chosen such that $u_N$, is some small percentage of $u_{eq}$ to ensure $u(t) \in (0,\ 1)$. The control law of (3.31), is then compared with a triangular carrier signal of desired frequency to generate PMW pulses for the converter's switch, resulting in a fixed frequency switching. The implementation scheme of the proposed PWM based SMC is shown in Figure 3.3 and simulation studies for the same are presented in the Section 3.2.3.

#### *(a) Existence of sliding mode*

The detailed proof of the existence of sliding mode for the reaching dynamics of (3.30) has been given in Chapter 2.

### 3.2.3 Simulation Studies

In this section, simulation studies are presented to validate the effectiveness of the proposed controllers, to mitigate CPL induced negative impedance instabilities in the dc buck converter system of Figure 3.1. The system with the proposed discontinuous and PWM based SMCs was simulated in $MATLAB/SIMULINK^{TM}$ with a discrete step size of 10 $\mu s$. The values of the converter parameters and nominal values of load used in the simulation studies were: $L = 2\ mH$, $C = 1000\ \mu F$, $E = 380\ V$, $x_{2ref} = 220\ V$, $P = 350\ W$, and $R_L = 322.67\ \Omega$. Inductor current reference $i_{Lref}$ was estimated using $i_{Lref} = v_{ref} i_{load}/v_C$. First, simulation studies with discontinuous SMC are presented, followed by simulation studies with PWM based SMC.

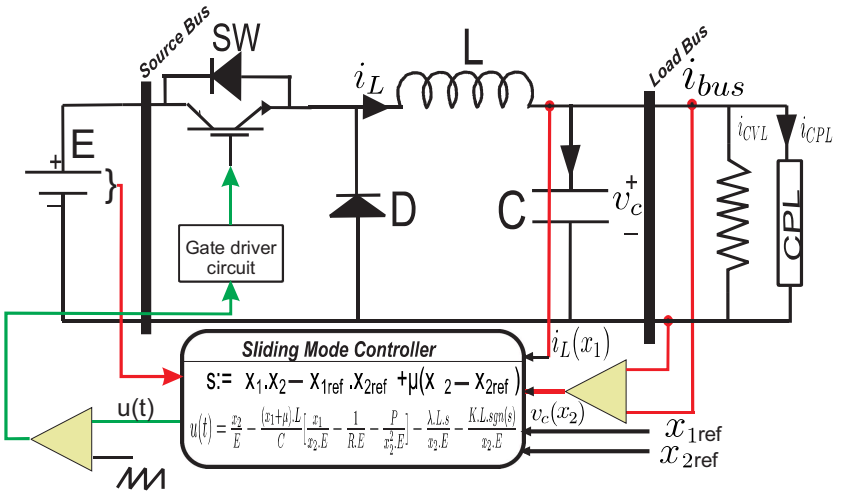


**Figure 3.3 :** Implementation scheme of the proposed PWM based SMC for buck converter feeding a mixed load

***(a) Simulation studies with discontinuous SMC***

The simulation studies of the buck converter system controlled through the proposed discontinuous SMC was carried out with $\mu = 200$. The control law (3.6) has been modified, keeping in view its practical implementation to avoid very high frequency switching and high switching losses. In order to limit the switching frequency, hysteresis band $h = 5$ has been used in the modified control law as

$$u := \frac{1}{2}(1 - sgn(s)) = \begin{cases} 0 & \text{if } s > h \\ 1 & \text{if } s < -h \\ u_p & \text{if } -h < s < h \end{cases} \tag{3.33}$$

where $u_p$ is the previous value of the control input. The region of existence corresponding to

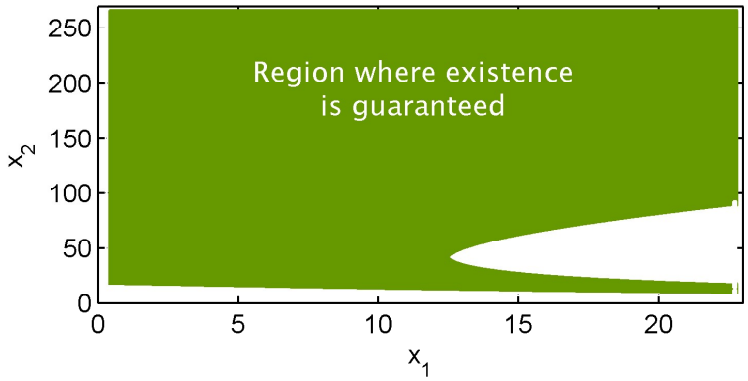


**Figure 3.4 :** Region of existence for simulated case (shaded in green) of buck converter system

the above simulation case with reference to (3.13) and (3.17), is shown in Figure 3.4. Simulation results corresponding to start-up and transient response are given in Figures 3.5-3.8.

Figure 3.5, shows the start-up response of the system in terms of the output voltage, the inductor current, switching function and control input. It can be seen from Figure 3.5(a), that the output voltage reaches its reference value in less than 5 *ms* with negligible steady

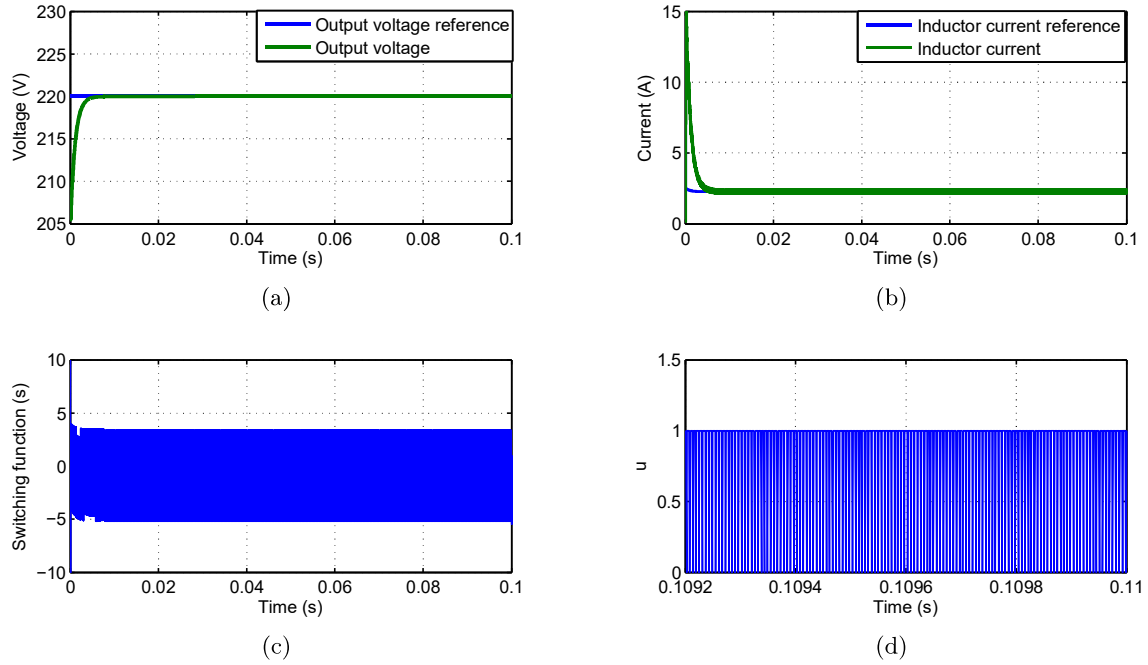


**Figure 3.5 :** Simulated start-up response with the discontinuous SMC: (a) Output voltage; $(b)$ Inductor current; $(c)$ Switching surface; and $(d)$ Control input. $(E = 380\,V, P = 350\,W, R = 322.67\,\Omega,\ x_{2ref} = 220\,V$ and $\mu = 200)$

state error. The inductor current (Figure 3.5(b)) tracks its reference value perfectly, but has high start up value. This is quite natural keeping in view the I-V characteristics of the CPL (voltage is small at the start-up which results in the high value of the inductor current). It is apparent from Figure 3.5(c), switching function remains within a band. The control input is shown in Figure 3.5(d).

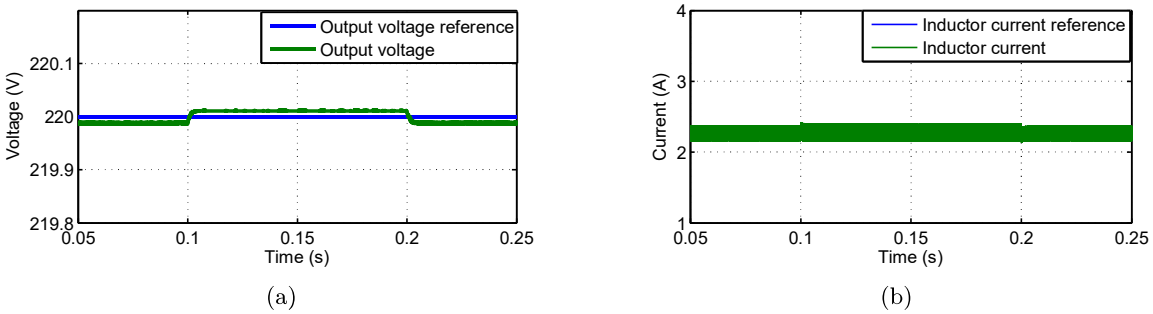


**Figure 3.6 :** Simulated transient response with the discontinuous SMC: (a) Output voltage; $(b)$ Inductor current. (When input voltage is increased by 30% at $t = 0.1\ s$ and is restored at $t = 0.2\ s$)

The transient response of the output voltage and the inductor current to a 30% increase in the input voltage is shown in Figure 3.6. It can be seen that the output voltage increases by less than $0.05\ V$ $(0.023\%)$ and the inductor current is also negligibly affected by this step change. The transient response of the output voltage and the inductor current to a step

decrease of 30% in the input voltage is given in Figure 3.7. This reduction in the input causes the output voltage to drop only by less than 0.05 $V$. In response to the decrease in the input voltage, the inductor current ripple decreases as shown in Figure 3.7(b).

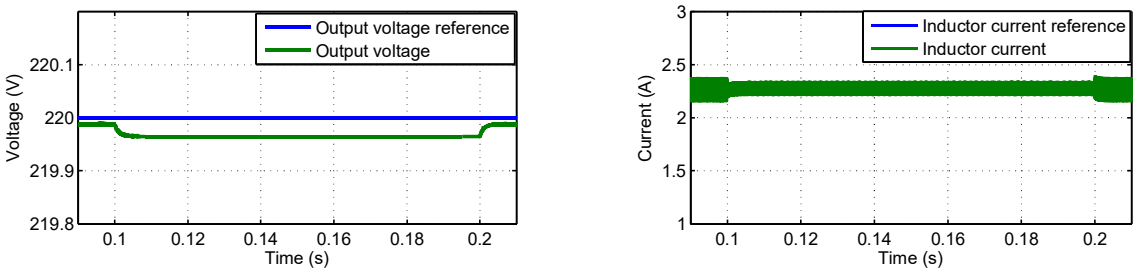


**Figure 3.7 :** Simulated transient response with the discontinuous SMC: (a) Output voltage; $(b)$ Inductor current. (When input voltage is decreased by 30% at $t = 0.1\ s$ and is restored at $t = 0.2\ s$)

In response to the increase in the CPL power from 350 $W$ to 500 $W$, keeping the resistive load fixed, the output voltage is maintained at its steady state value of $\approx 220\ V$ and the inductor current instantly follows its changed references (Figure 3.8).

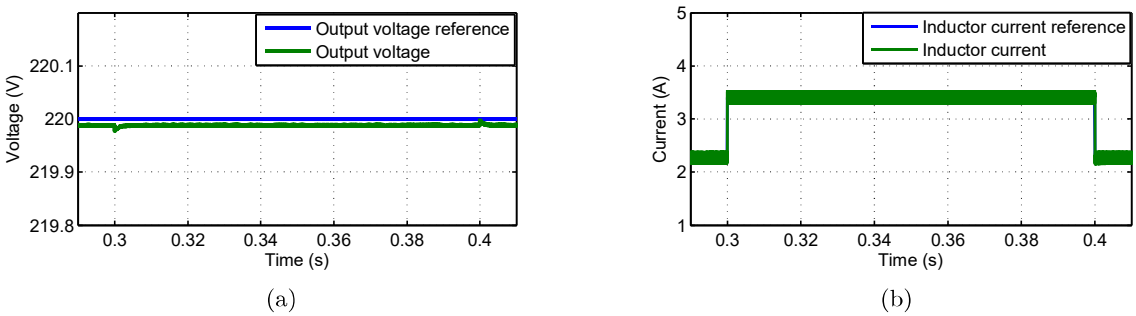


**Figure 3.8 :** Simulated transient response with the discontinuous SMC: (a) Output voltage; $(b)$ Inductor current. (When CPL power is increased from 350 $W$ to 500 $W$ at $t = 0.3\ s$ and is restored at $t = 0.4\ s$, keeping resistance $R_L$ constant)

***(b) Simulation studies with PWM based SMC***

In this section, validation of the performance of the proposed PWM based SMC is presented through simulation studies, when it is controlling the buck converter feeding a mixed load. All the operating conditions and system parameters were kept same as in the case of the discontinuous SMC. The parameters of the PWM based SMC used in the simulation studies are provided in Table 4.1. The simulation results under various operating conditions are given in the Figures 3.9-3.12.

Figure 3.9, shows response of the output voltage, the inductor current, switching function and control input during start-up and steady-state operation. Although in this case the output voltage and the inductor current, shown in Figures 3.9(a) and 3.9(b), take 10 *ms* to reach their steady state as compared to 5 *ms* with the discontinuous SMC case (Figures 3.5(a) and 3.5(b)), but are able to track their references with negligible error. The average value of

**Table 3.1 :** Parameters of the proposed PWM based SMC for buck converter

| Parameter | Value |
|---|---|
| $\mu$ | 200 |
| $\lambda$ | $1X10^5$ |
| $Q$ | $3X10^8$ |
| Switching frequency ($f_s$) | 20 $kHz$ |

the switching function (Figure 3.9(c)) is close to zero. Figure 3.9(d), shows generated PWM pulses for the converter switch.

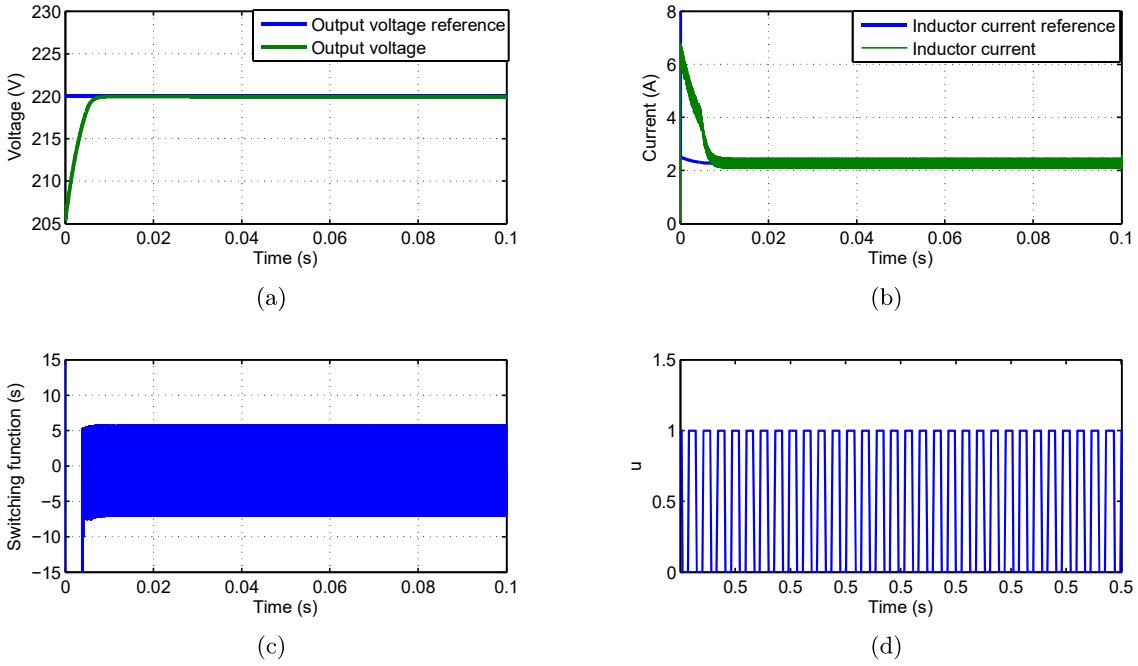


**Figure 3.9 :** Simulated start-up response with the PWM based SMC: (a) Output voltage; $(b)$ Inductor current; $(c)$ Switching surface; and $(d)$ Control input. $(E = 380\,V, P = 350\,W,\ R_L = 322.67\,\Omega, x_{2ref} = 220\,V)$

The transient responses corresponding to the 30% step increase and decrease in the input voltage are shown in Figure 3.10 and Figure 3.11 respectively. It can be seen that, in response to the $\pm 30\%$ change in the input voltage, the output voltage changes by only $\pm 0.05\,V$. The inductor current is also maintained at its reference value except for the negligible transients at the instances of step changes.

Figure 3.12, shows transient response corresponding to the step increase in the CPL power from $350\,W$ to $500\,W$ at $t = 0.3\,s$ and back to its previous value at $t = 0.4\,s$, keeping CVL resistance $R_L$ to a fixed value. It is evident from the plot that the output voltage is maintained to its reference value, and a very small magnitude transients are seen at the instances of step changes. The inductor current follows its changed references instantly.

The above simulation studies validate the performance of the discontinuous and PWM based SMCs under various operating conditions. Both the controllers ensure desired stable

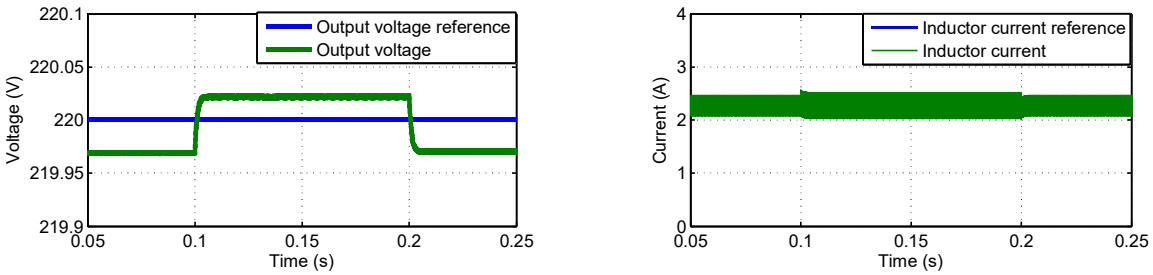


(a) (b)

**Figure 3.10 :** Simulated transient response with the PWM based SMC: (a) Output voltage; $(b)$ Inductor current. (When input voltage is increased by $30\%$ at $t = 0.1\ s$ and is restored at $t = 0.2\ s$)

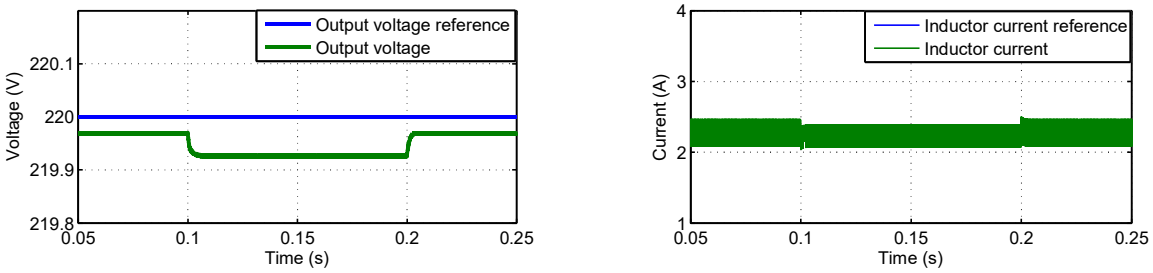


(a) (b)

**Figure 3.11 :** Simulated transient response with the PWM based SMC: (a) Output voltage; $(b)$ Inductor current. (When input voltage is decreased by $30\%$ at $t = 0.1\ s$ and is restored at $t = 0.2\ s$)

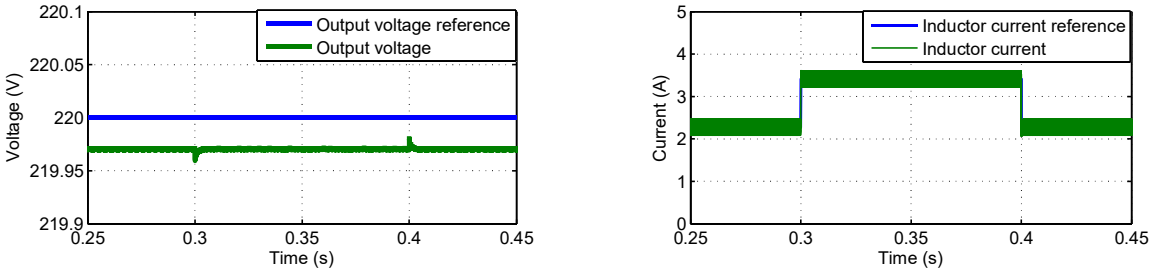


(a) (b)

**Figure 3.12 :** Simulated transient response with the PWM based SMC: (a) Output voltage; $(b)$ Inductor current. (When CPL power is increased from $350\ W$ to $500\ W$ at $t = 0.3\ s$ and is restored at $t = 0.4\ s$, keeping resistance $R_L$ constant)

output voltage and fast transient performance (settling time of $< 1$ *ms*).

### 3.2.4 Experimental Validation

In this section, experimental validation of the proposed discontinuous and PWM based SMCs is presented using a laboratory prototype of dc/dc buck converter feeding a mixed load. An image of the experimental setup is shown in Figure 3.13, consisting of a dc/dc buck converter, programmable dc load, Field Programmable Gate Arrays (FPGA) card, Gate driver card, input dc supply, and the dc supply for sensors. In order to realize the controllers the input voltage, output voltage, inductor current, and load current of the converter have been sensed using voltage sensors ($LEM\ LV25-1000$) and current sensors ($ACS709$). The controllers have been realized using National Instruments (NI) General Purpose Inverter Control (GPIC) card, (NI sb-RIO 9606), programmable through Labview software. The different waveforms of the variables of importance have been captured using DPO for monitoring and subsequent analysis. The specifications of the experimental prototype and the nominal values of the system variables are described in Table 4.2.

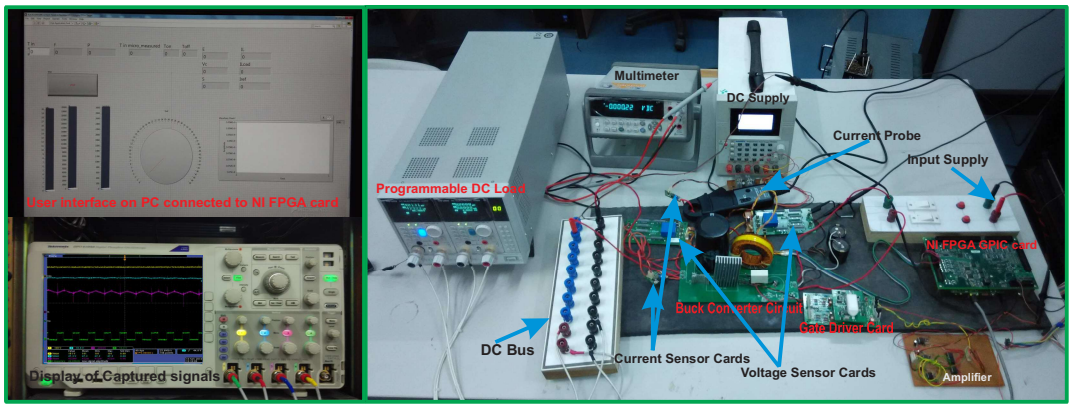


**Figure 3.13 :** An image of the experimental setup of buck converter feeding a mixed load

**Table 3.2 :** Specifications of the experimental setup of buck converter system

| Parameter | Value |
|---|---|
| Nominal output voltage, $V_o$ | 48 $V$ |
| Nominal input voltage, E | 100 $V$ |
| L & ESR | 2 $mH$ & 0.224 Ω |
| C & ESR | 1000 $\mu F$ & 0.185 Ω |
| CPL power, P | 200 $W$ |
| Resistive load, $R_L$ | 208 Ω |
| IGBT (FGL40N120) | 1200 $V$, 40 $A$ |
| Diode (MUR 1560) | 300 $V$, 15 $A$ |
| Switching frequency, $f_s$ | 25 $kHz$ (for PWM version) |

The experimental results have been captured under three operating conditions: (1) steady-state operation with nominal values, (2) transient response corresponding to a 25% reduction in the input voltage, and (3) transient response corresponding to a reduction in the CPL power from nominal value to zero, keeping CVL component of load unchanged. The changes in the input voltage were introduced by manual rotation of the knob of dc power supply. On the other hand, changes in CPL were introduced in the form of steps, to the used

programmable dc load.

### *(a) Experimental validation of the discontinuous SMC*

As discussed, the switching frequency of the buck converter when controlled through discontinuous SMC can be very high, resulting in increased switching losses. Therefore, to limit highest switching frequency and to reduce the switching losses, a hysteresis band was used in the practical implementation. Furthermore, the gate driver card also limits the upper switching frequency. It can pass upto 50 $kHz$, but the switching is still of variable frequency. A value of 40 was used for the controller parameter $\mu$.

The experimental results under the above mentioned operating conditions are given in Figure 3.14. Figure 3.14(a), shows the output voltage of 48.6 $V$(slightly higher than the reference of 48 $V$), corresponding to the Operating Condition: 1. The input voltage, the inductor current, and PWM switching pulses are also shown in this figure. The output voltage reduces only by $<$ 2% in response to 25% reduction in the input voltage, corresponding to the Operating Condition: 2 and recovers to its previous value when input voltage is restored (Figure 3.14(b)). Figure 3.14(b), also shows that the inductor current ripple reduces with the reduction in the input voltage, which confirms the simulation result obtained in Figure 3.7(b). When the CPL power is changed corresponding to the Operating Condition: 3, the output voltage reduces only by $<$ 1% and returns to its previous value when CPL power is again increased to 200 $W$ (Figure 3.14(c)). Under all three operating conditions, the proposed discontinuous SMC ensures regulation of the output voltage (within $\pm$3.125%) and stabilization against CPL induced negative impedance instabilities.

### *(b) Experimental validation of the PWM based SMC*

The PWM based SMC has also been validated through experimental results obtained under the same above mentioned operating conditions. The values of the controller parameters were: $\mu = 40$, $\lambda = 1500$ and $Q = 20000$. The obtained results are shown in Figure 3.15.

It can be seen from Figure 3.15(a), that the output voltage perfectly tracks its reference value 48 $V$, corresponding to the Operating Condition: 1. The input voltage, the inductor current, and PWM switching pulses are also shown in this figure. The output voltage reduces and shows a transient disturbance, for the duration, when input voltage was under change corresponding to the Operating Condition: 2, and recovers to its previous value, when the input voltage becomes stable (Figure 3.15(b)). One of the main cause behind the transient disturbance is the method to introduce variations in the input voltage. Furthermore, corresponding transient disturbance is also visible in the inductor current waveform. The transient response corresponding to the Operating Condition: 3, shown in Figure 3.15(c), shows that in response to the removal of CPL, the output voltage increases by less than 2% , and returns to its previous value when CPL power is again increased to 200 $W$. It demonstrates that the PWM based SMC also performs well under the above mentioned operating conditions, except for its sensitivity to the slow variations in the input voltage. The above simulation studies and experimental results validate the performance of the proposed sliding mode controllers to mitigate destabilizing effects of the CPLs and to ensure tight regulation of the output voltage of the buck converter feeding mixed load. When compared to the discontinuous SMC, the PWM based SMC results in longer settling time and is sensitive to slow variations in the input voltage.

## 3.3 SUMMARY

In this chapter mitigation of CPL induced negative impedance instabilities in a dc/dc buck converter feeding a combination of CPL and CVL, which is generic case, has been presented through SMC approach. A nonlinear switching function based discontinuous and PWM

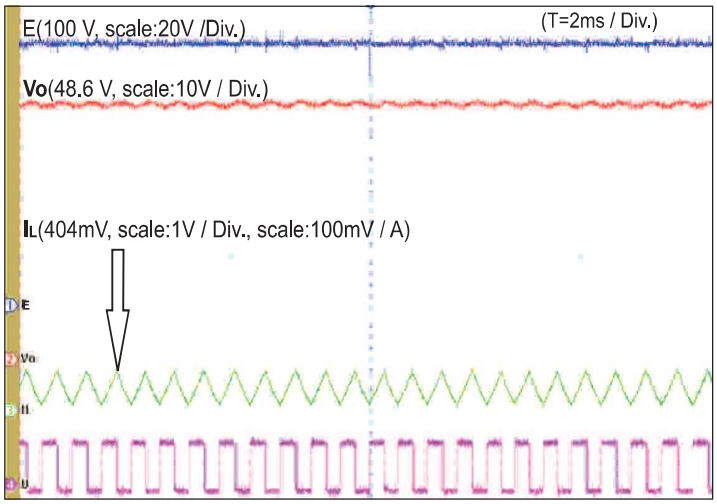


(a)

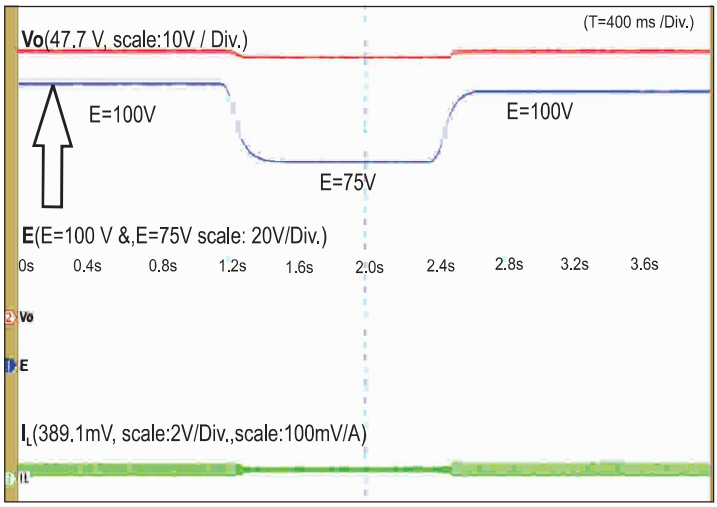


(b)

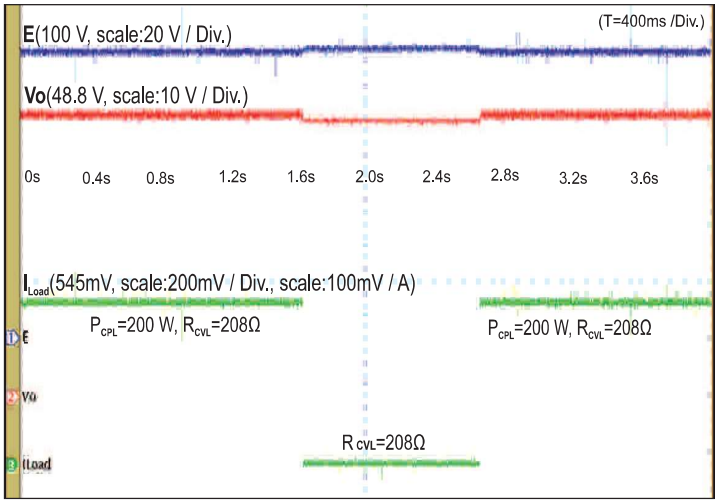


(c)

**Figure 3.14 :** Experimental results with the discontinuous SMC: $(a)$ Steady-state operation corresponding to the Operating Condition: 1; $(b)$ Transient response corresponding to the Operating Condition: 2; $(c)$ Transient response corresponding to the Operating Condition: 3

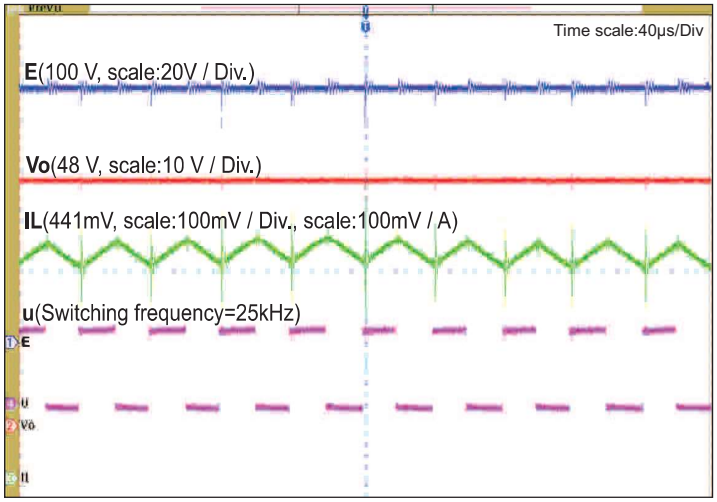


(a)

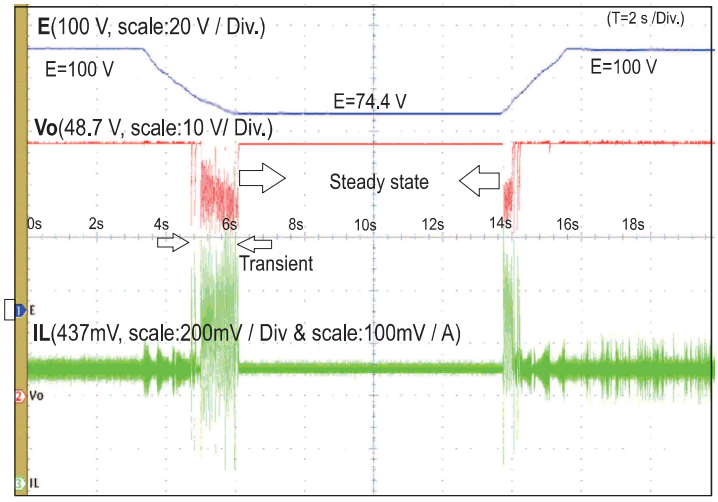


(b)

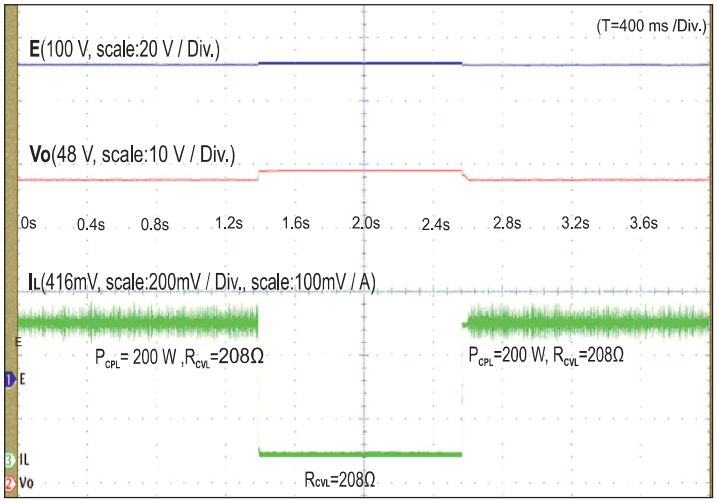


(c)

**Figure 3.15 :** Experimental results with the PWM based SMC: $(a)$ Steady-state operation corresponding to the Operating Condition: 1; $(b)$ Transient response corresponding to the Operating Condition: 2; $(c)$ Transient response corresponding to the Operating Condition: 3

versions of SMC have been proposed. The existence of sliding mode, stability of switching surface have been established, and the condition on the total power to ensure the stability has also been derived. The steady-state and transient performance of the controllers have been validated through simulation studies, which has been further validated through experimental results using a laboratory prototype of dc/dc buck converter feeding a mixed load. The controllers are realized through NI FPGA card programmed using NI LabView software. Both controllers are robust with respect to the sufficiently large variations in the input voltage and load. However, it was found from experimental results that PWM based SMC is sensitive to the slow variations in the supply. Furthermore, the controllers ensure tight regulation of the output voltage and system stability under different operating conditions. In the next chapter, mitigation of the destabilizing effects of CPLs in non-isolated topology dc/dc buck-boost converters using SMC approach will be addressed.

...